PACE-2023
International Congress on the Phenomenological Aspects of Civil Engineering

PACE-2023
International Congress on Phenomenological Aspects in Civil Engineering

Research Article
20-23 June 2023

Investigation of Dynamic Characteristics of Blast Effects on Reinforced Concrete Structure Models with Different Geometrical Properties

Fatma Önalan[1], Fezayil Sunca[2], Ahmet Can Altunışık*[,3]
[1] *Ankara Water and Sewerage Administration, 06050 Ankara, Turkey*
[2]*Department of Civil Engineering, Faculty of Engineering, Sivas Cumhuriyet University, 58140 Sivas, Turkey*
[3]*Department of Civil Engineering, Faculty of Engineering, Karadeniz Technical University, 61080 Trabzon, Turkey*
Corresponding Author E-mail:ahmetcan8284@hotmail.com

Keywords

Explicit Analysis,
Buildings.,
Blast Load,
Explosives.,
Concrete strength..

Abstract

Engineering structures such as buildings, highways, hospitals and bridges are all necessary structures for people to maintain their basic lives. In recent years, with the development of technology and the increase in wars, we have been witnessing the effects of the explosion phenomenon that occurred as a result of accidents or terrorist attacks in daily life. Within the scope of this study, the effect of explosions occurring in different scenarios around a building was examined. Within the scope of the study, a parametric study was carried out on a total of 72 scenarios using two different building models, 6 different explosive weights and 6 different concrete strength classes, and the dynamic responses of the elements constituting the building were examined. When the data obtained as a result of the studies are examined, it has been determined that the strength class of the concrete material, which constitutes the majority of the building, the explosive weight and distance, as well as the presence of the hollow geometry in the structure are of great importance and play an active role. Explosion resistant structures can be constructed using the parameters explained in the light of the results obtained.

1. Introduction

With the Second World War, it is seen that the analytical and experimental studies on the effects of explosive types and those who tried them, on the behaviors caused by explosions in the scientific field, also took place in the literature. The explosion effect from the 1950s to the present continues to increase with the processes going through them and the analytically advancing and future technology. It shows that it pays more and more attention to the consequences of terrorist bomb attacks, especially in the last twenty years.

Empirical, experimental and numerical studies have been carried out by many scientists to determine the dynamic responses of structures as a result of the explosion event. First of all, in the 1950s, Newmark (1953) [1] presented suggestions for the design of structures resistant to explosion effects, determined the calculation steps, and defined the numerical relation that determines the explosion load pressure function. In later studies [2,3,4,5,6] various empirical formulas were developed to measure the pressure values caused by the explosion on the structural element, and numerical studies related to the subject were continued. Although the obtained numerical relations are useful in reading the pressure effect on the building element, they are not sufficient for today.

On the other hand, when the experimental studies on reinforced concrete structures are examined, almost all of the studies were carried out on only a single load-bearing element [7,8,9]. The data obtained from experimental studies, on the other hand, are limited in the literature due to the complexity of the explosion phenomenon and limited measurability [10,11].

In the literature, in the measurement of dynamic responses of reinforced concrete structures; Finite Element (FE) method in building type structures [12,13,14,15,16], in studies for retaining walls [17,18], in bridges and dams [19,20,21] handled using. When the aforementioned studies are examined, using the vibrations caused by the explosive material types and the ground movements caused by the explosion, the dynamic responses of the structural bearing elements, reliability analyzes, load residual capacity, collapse mechanisms, etc., under variable parameters such as explosive weight and distance, responses have been evaluated.

Scope of this study, the effects of explosive weight and distance on different concrete strength classes on a reinforced concrete single-storey building type building model with two different geometrical properties are discussed. In the first stage of the study, a numerical modeling of a structure built according to the conditions of the Turkish Earthquake Code (2018) [22] was carried out on the ANSYS Workbench [23] program in order to measure the reactions to occur in the explosion event in a partially confined environment. Subsequently, the created model was transferred to ANSYS Autodyn [24] for explicit analysis within the ANSYS program. Obtained results are given comparatively on the graph.

2. Blast Theory

The detonation of high-intensity explosives leads to blast waves. The blast waves produce a shock wave effect that spreads from the explosion center to the atmosphere with hemispherical form. After the shock wave releases from the center of the explosion, it reaches the maximum pressure (P_{so}) and speed value in a short time like a millisecond. As the shock wave moves away from the explosion center, the surface area expands and the pressure value gradually decreases. This process continues until a balance is achieved with the air surrounding the shock wave. This process is defined as the positive phase duration (to). During the propagation of the shock wave, the pressure value in the region behind of the shock wave falls below the ambient pressure and creates negative pressure (P^{-}_{so}). This process, which creates a vacuum effect, is defined as the negative phase duration (t-o). The time-history graph of blast wave pressure is given in Fig.1. Examined in the literature, generally duration of the blast approximately 2,5-3 milliseconds and value of P_{so} can reach to big overpressures.

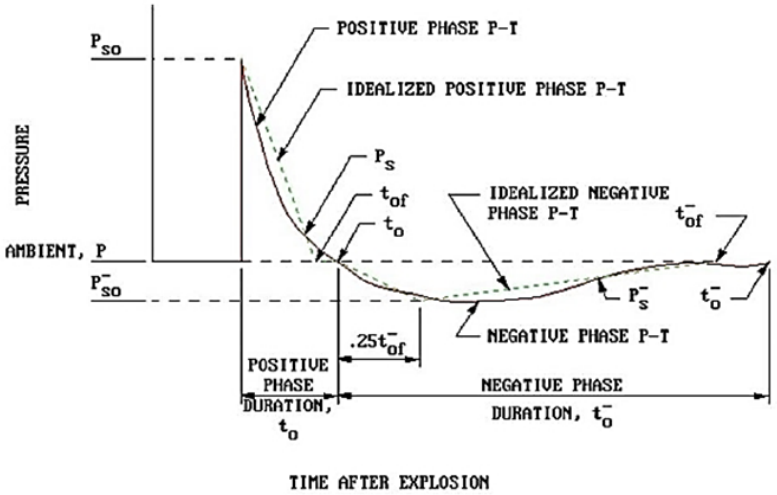

Figure 1. Pressure wave-distance interaction related to blasting

3. Finite Element Model

In this research, two building models were selected in this study. In Model I, gas escape is easily provided from the door and window openings on all facades, and in Model II, the rear facade walls of the building are assumed to be void-free to prevent explosion pressures leaving the building. The length of the building is 9000 mm (X axis), width is 6200 mm (Z axis), height is 3000 mm (Y axis), foundation depth and cantilever are determined as 500 mm. The columns cross-section was selected as 600 × 300 mm, beams cross section was 500 × 300 mm, and the slabs thickness was 120 mm. brick wall properties was selected, thick 100 mm and high 2500 mm. The slab thickness is selected as 12 cm. The buildings contain six columns and the cross-section dimensions of the columns is 30 × 60 cm. For all columns, the confinement bars are φ8/100 mm (confinement zone), φ8/195 mm (other regions) and longitudinal bars are 6φ20. The dimensions of the beams are 30 × 50 cm. The reinforcing bars of beams are 6φ16. For all beams, confinement bars are determined as φ8/100 mm (confinement zone) and φ8/200 mm (other regions). B420C (f_{yk} =420 MPa) steel class is selected for all load-bearing elements. The walls are constituted using brick elements that are 45% hollow ratio according to the Turkısh Earthquake Code. The concrete material properties used in the finite element model of buildings are summarized of Table 1 and other materials properties given Table 2 respectively.

Table 1. Concrete material properties finite element of buildings

Concrete strength						
	C25/30	C30/37	C35/45	C40/50	C45/55	C50/60
fc (MPa)	25.00	30.00	35.00	40.00	45.00	50.00
Poisson Ratio				0.20		

Table 2. Material properties finite element of buildings

Material Component	Material Type	Density (g/cm^3)	Compressive trength (MPa)
Reinforcing Bar	B420C	2.40	420.00
Infill Wall	Brick	0.69	5.00

The FE models of the buildings are constituted in ANSYS Workbench software. To perform explicit analyses of the buildings, the FE models are transferred into ANSYS Autodyn software. The Lagrange theory is used for solid elements. Air volume and TNT explosives are modeled according to Euler's theory.

The FE models of the buildings are given in Fig. 2. The detonation is a phenomenon that occurs in a very short time period. To observe the differences in pressure change, the analysis time should be chosen appropriately. The analyses times are considered as 3ms and the increment interval of 0.01ms. In the blasting analyses, 29 gauge points are selected to monitor the blasting responses of the buildings. These gauge points are specified various important regions such as joints of load-bearing elements, brick walls, and structural elements-infill wall interaction regions to determine the blasting responses of the different facades of buildings. These selected gauge points are given in Fig. 3.

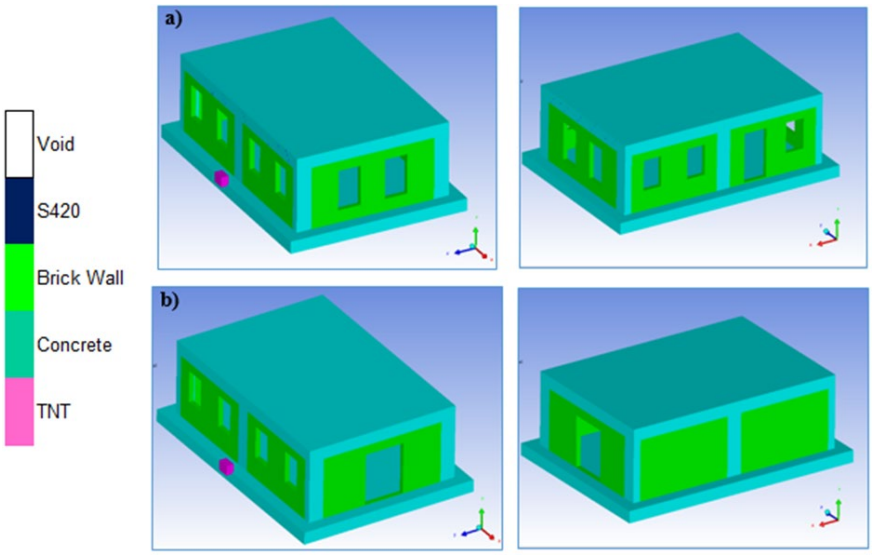

Figure 2. Finite element models of the building models (a. Model I, b. Model II)

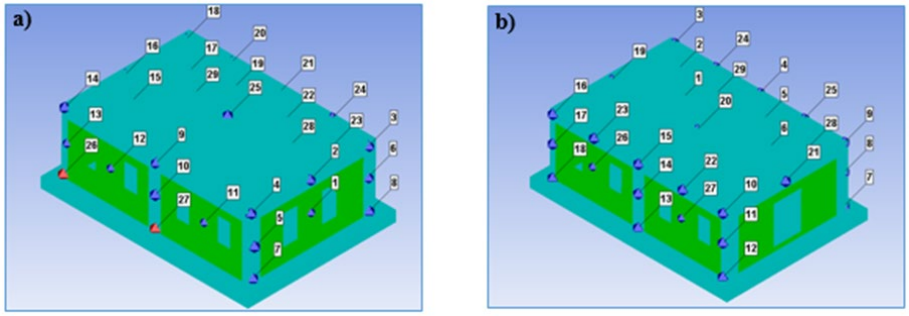

Figure 3. Gauge points (a. Model I, b. Model II)

4. Explicit Analysis

In the analysis of structures, the maximum responses obtained from numerical studies are generally guiding in our understanding of structural behavior. Therefore, the critical measurement points at which maximum responses are obtained in structural elements and infill walls were determined to compare the results of 72 explicit analyzes. The maximum responses of the structural elements were obtained from gauge 27 for Model 1 and from gauge 13 for Model 2. Also, gauge 12 and gauge 26 are critical points for the infill walls of Model 1 and Model 2, respectively. The common feature of these gauge points is that they are located on the building facades and are closest to the explosion center. The four critical gauge points chosen for both structural members and infill walls are given in Figure 4.

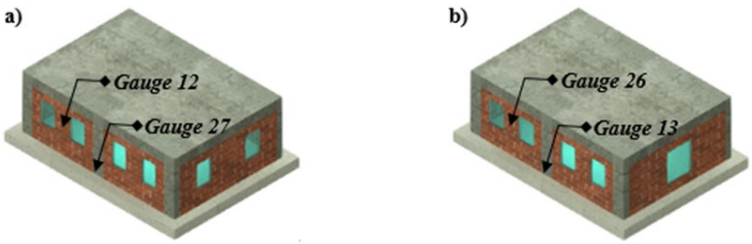

Figure 4. Critical gauge points at the front façade of models (a. Model I, b. Model II)

To determine the effects of concrete strength, TNT charge weight, and the opening ratio in infill walls on the blasting responses, the peak pressures are comparatively investigated. Figs. 5-8 present the time-history of peak pressures obtained from the critical gauge points on the load-bearing elements and infill walls of Model 1 and Model 2.

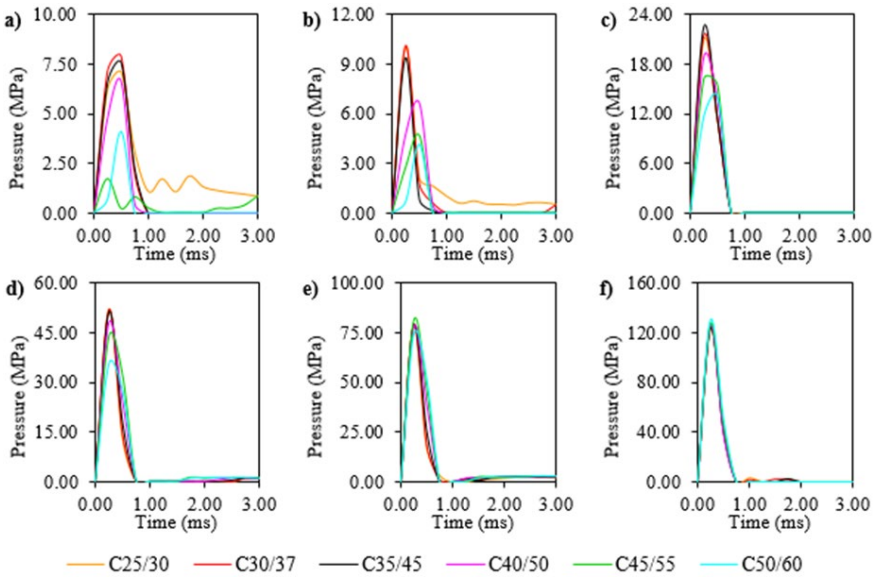

Figure 5. The time-histories of peak pressures obtained from the load-bearing elements of Model 1 (charge weight; a. 5kg, b. 10kg, c. 25kg, d. 50kg, e. 100kg, f. 200kg)

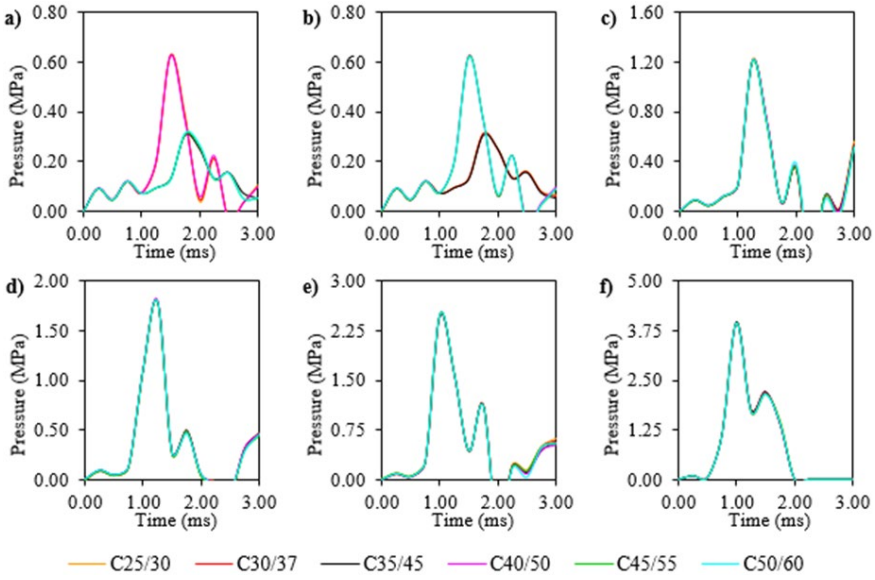

Figure 6. The time-histories of peak pressures obtained from the infill walls of Model 1 (charge weight; a. 5kg, b. 10kg, c. 25kg, d. 50kg, e. 100kg, f. 200kg)

The maximum differences between the peak pressures of Model 1 and Model 2 due to the openings in infill walls are determined as 64.45% for 5kg TNT, 68.95% for 10kg TNT, 34.54% for 25kg TNT, 18.86% for 50kg TNT, 11.66% for 100kg TNT, and 13.26% for 200kg TNT.

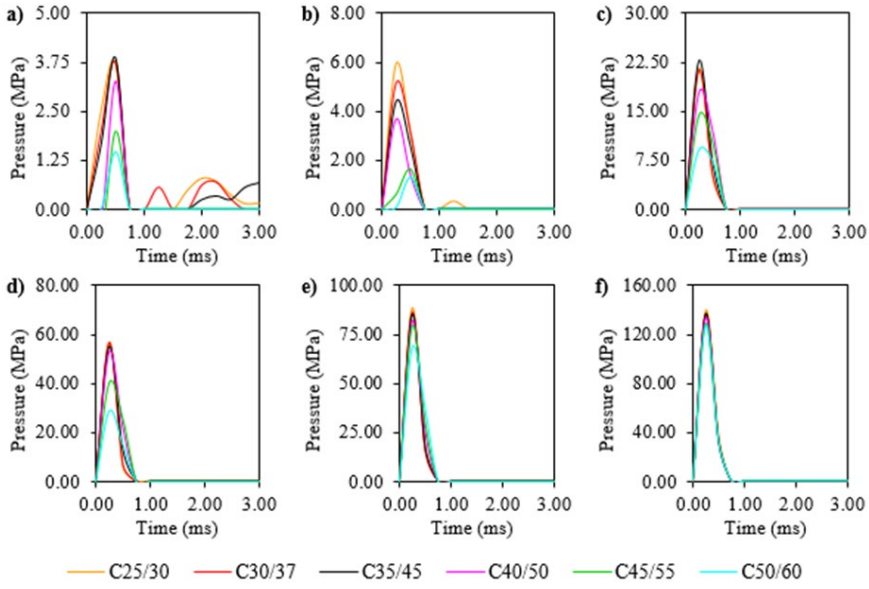

Figure 7. The time-histories of peak pressures obtained from the load-bearing elements of Model 2 (charge weight; a. 5kg, b. 10kg, c. 25kg, d. 50kg, e. 100kg, f. 200kg)

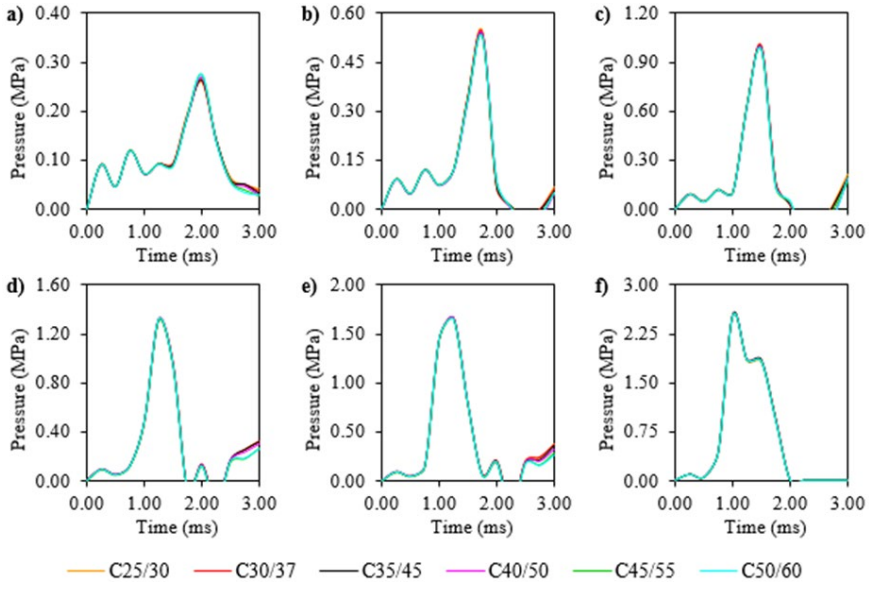

Figure 8. The time-histories of peak pressures obtained from the infill walls of Model 2 (charge weight; a. 5kg, b. 10kg, c. 25kg, d. 50kg, e. 100kg, f. 200kg)

Figs. 9-10 comparatively present the time-history of displacements obtained from the critical gauge points on the load-bearing elements for each model. In Model 1, the displacements of the structural elements increase from 1.88mm to 85.48mm for C25/30, 1.89mm to 84.65mm for C30/37, 1.95mm to 80.43mm for C35/45, 2.00mm to 75.11mm for C40/50, 1.82mm to 69.41mm for C45/55, and 1.48mm to 63.43mm for C50/60 with the increasing of explosive material weights from 5kg to 200kg. Similar upward trends are observed in Model 2 depending on the increase in the TNT weights. The increases in maximum displacements obtained from the structural elements of Model 2 are determined from 0.63mm to 99.54mm for C25/30, 0.79mm to 95.91mm for C30/37, 0.67mm to 92.73mm for C35/45, 0.74mm to 86.89mm for C40/50, 0.70mm to 80.55mm for C45/55, and 0.68mm to 75.60mm for C50/60. It is also observed from the Figs. 18, 20, and 22 that the maximum displacements of the infill walls increase by nearly 20.63 times for Model 1 and 22.21 times for Model 2 with the increase of weights of TNT from 5kg to 200kg.

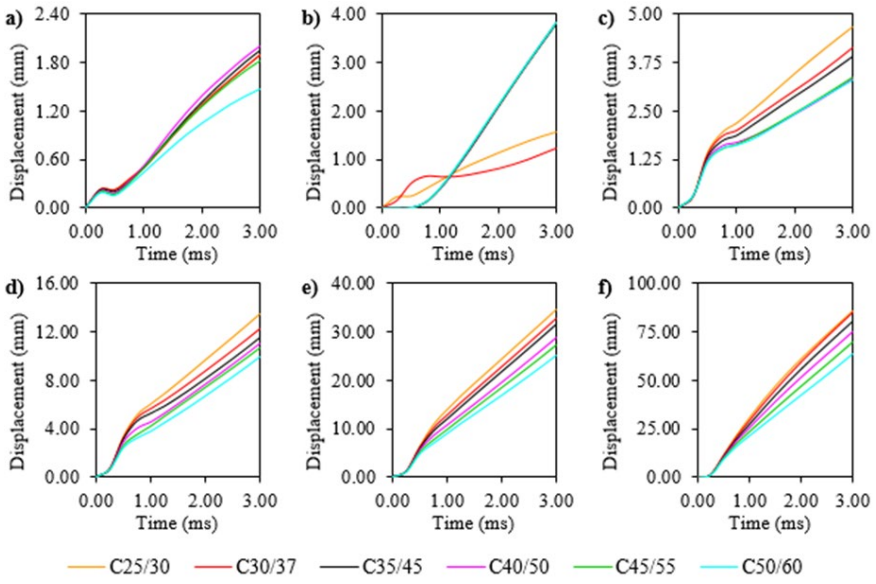

Figure 9. The time-histories of maximum displacements obtained from load-bearing elements of Model I (charge weight; a. 5kg, b. 10kg, c. 25kg, d. 50kg, e. 100kg, f. 200kg)

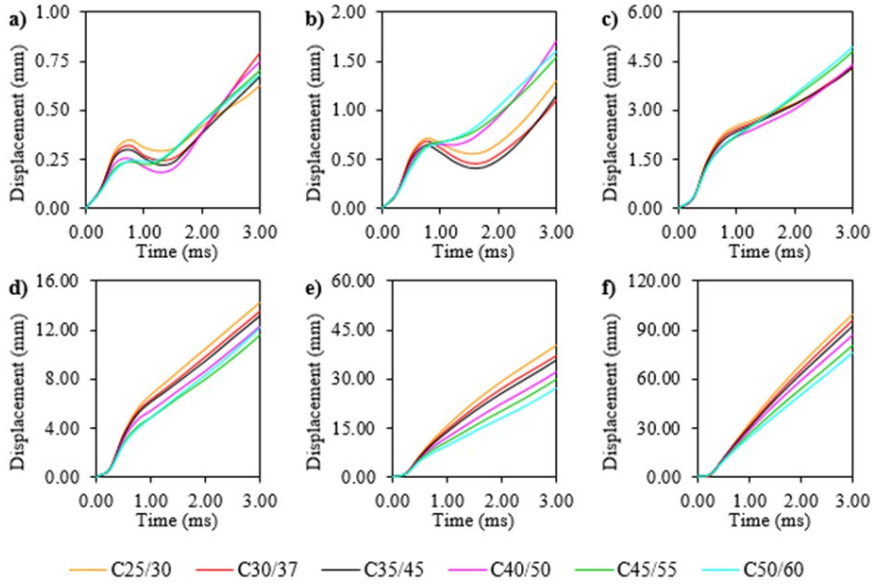

Figure 10. The time-histories of maximum displacements obtained from load-bearing elements of Model II (charge weight; a. 5kg, b. 10kg, c. 25kg, d. 50kg, e. 100kg, f. 200kg)

The released-total energies obtained from selected explosion material weights and absorbed-total energies by the air volume are plotted in Fig. 11. It can be seen from Fig. 11 that the released energies are determined as 0.18×1014μJ for 5kg TNT, 0.36×1014μJ for 10kg TNT, 0.90×1014μJ for 25kg TNT, 1.8×1014μJ for 50kg TNT, 3.6×1014μJ for 100kg TNT, and 7.2×1014μJ for 200kg TNT.

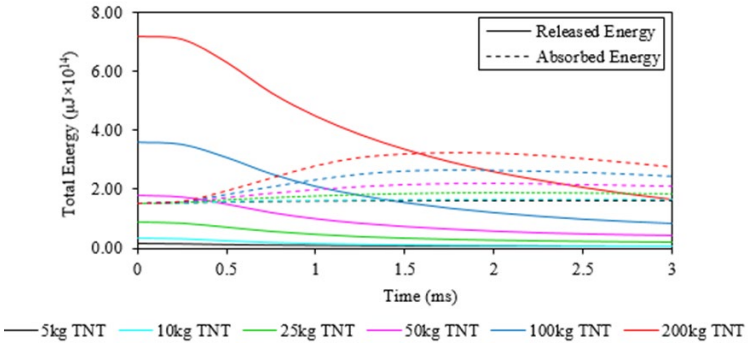

Figure 11. The time-histories of released energies by explosives and absorbed by air volume

5. Result and Discussions

As a result of the blasting analyses, the damage contour diagrams of Model 1 and Model 2 are plotted and are presented in Figs. 12 and 13. Similar damage distributions are observed in all blasting scenarios and concrete strengths, as the absorbed energies by the concrete and brick materials are negligible. Therefore, damage distributions of buildings exposed to different TNT explosives for the C25/30 and C50/60 concrete strengths are given in Figs. 14 and 15. With the increase in explosive weight, the damages increased significantly for both models. During the analyses, the damages on the load-bearing elements and infill walls are concentrated in gauge 27 and gauge 12 for Model 1 and gauge 13 and gauge 26 for Model 2, respectively. These gauge points are located on the façades of buildings and are closest to the explosion center.

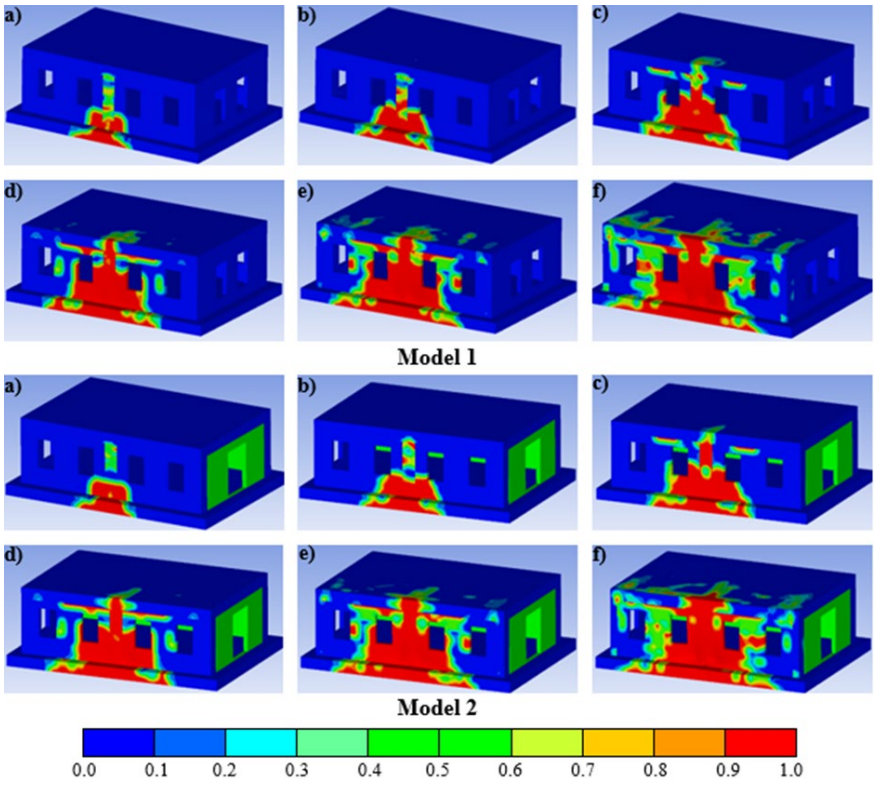

Figure 12. The damage contour diagrams obtained from C25/30 concrete strength for Model 1 and Model 2 (charge weight; a. 5kg, b. 10kg, c. 25kg, d. 50kg, e. 100kg, f. 200kg)

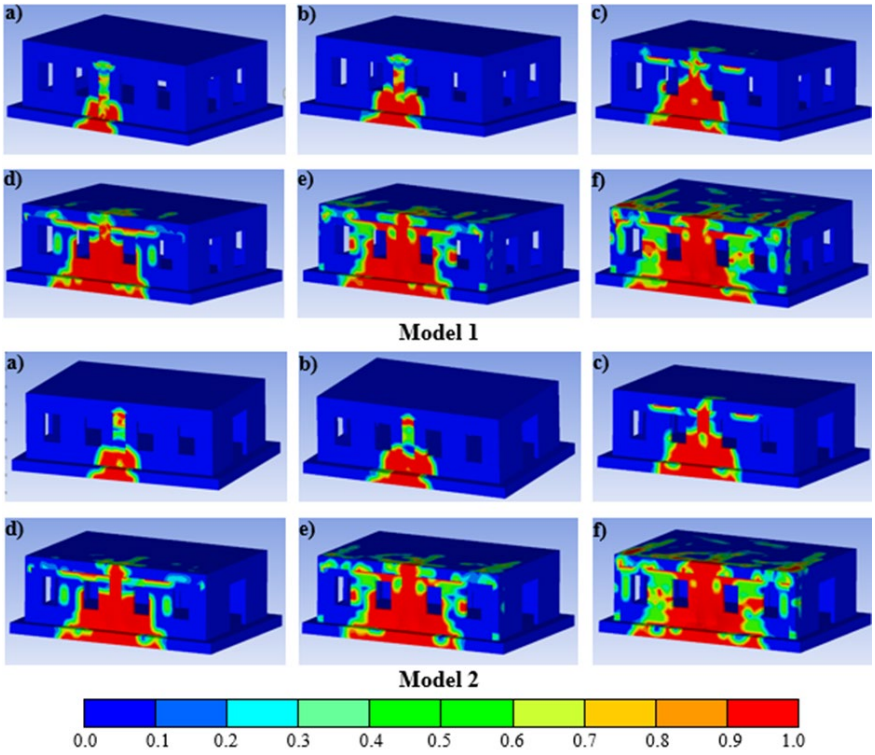

Figure 13. The damage contour diagrams obtained from C25/30 concrete strength for Model 1 and Model 2 (charge weight; a. 5kg, b. 10kg, c. 25kg, d. 50kg, e. 100kg, f. 200kg)

6. Conclusion

This study aims to assess the blasting responses and damages of RC buildings subjected to explosions. For this purpose, the explicit analyses are carried out by taking into account the effects of different TNT explosive weight, concrete strength, and different geometrical type of building. The blasting analyzes revealed that the wall openings caused crucial changes in the dynamic response of RC buildings. The differences of up to 68.95% were observed between the peak pressures obtained from the load-bearing elements of models due to window and door openings. The displacements of the load-bearing elements and infill walls were significantly affected by explosive weights. As the explosive weight increases, the displacements from both buildings also incrementally increase. As a result of the study carried out using 72 different scenarios, it was determinated that higher resistance against explosion and lower displacements were obtained in structures with hollow geometric structure and high strength concrete class.

Declaration of Conflict of Interests

The authors declares that there is no conflict of interest. They have no known competing financial interests or personal relationships that could have appeared to influence the work reported in this paper.

References

[1.] N.W.Newmark, An Engineering Approach to Blast Desingn. American Society of Civil Engineers (1953).

[2.] Brode, H.L.: Numerical solutions of spherical blast waves. J. Appl.Phys. 26(6), 766–775 (1955)

[3.] Henrych, J.; Major, R.: The dynamics of explosion and its use. Elsevier, Amsterdam (1979)

[4.] Kingery, C.N.; Bulmash, G.: Air blast parameters from TNT spherical air burst and hemispherical burst, technical report ARBRL-TR02555: AD-B082 713. US Army Ballistic Research Laboratory Aberdeen Proving Ground, Maryland (1984)

[5.] Kinney, G.F.; Graham, K.J.: Explosive shocks in air. Springer Publishing Company, Berlin (1985)

[6.] Mills, C.A.; The design of concrete structure to resist explosions and weapon effects. In: Proceedings of the 1st international conference on concrete for hazard protections. Edinburgh, 27–30 Sept 1987, pp. 61–73.

[7.] Codina, R.; Ambrosini, D.; de Borbón, F.: Experimental and numerical study of a RC member under a close-in blast loading. Eng.Struct. 127, 145–158 (2016). https://doi.org/10.1016/j.engstruct.2016.08.035

[8.] Dua, A.; Braimah, A.; Kumar, M.: Experimental and numerical investigation of rectangular reinforced concrete columns under contact explosion effects. Eng. Struct. 205, 109891 (2020). https://doi.org/10.1016/j.engstruct.2019.109891

[9.] Liu, L.; Zong, Z.; Ma, Z.J.; Qian, H.; Gan, L.: Experimental study on behavior and failure mode of psrc bridge pier under close-in blast loading. J. Bridg. Eng. 26(2), 04020124 (2021). https://doi.org/10.1061/(asce)be.1943-5592.0001662

[10.] Heggelund, S.; Brekken, K.; Ingier, P.; Christensen, S.O.: Global response of a three-story building exposed to blast loading. Multidiscip. Digit. Publ. Inst. Proc. 2(8), 386 (2018). https://doi.org/10. 3390/ICEM18-05211

[11.] Norén-Cosgriff, K.M.; Ramstad, N.; Neby, A.; Madshus, C.: Building damage due to vibration from rock blasting. Soil Dyn. Earthq. Eng. 138, 106331 (2020). https://doi.org/10.1016/j.soildyn.2020. 106331

[12.] Jayasooriya, R.; Thambiratnam, D.P.; Perera, N.J.; Kosse, V.: Blast and residual capacity analysis of reinforced concrete framed buildings. Eng. Struct. 33(12), 3483–3495 (2011). https://doi.org/10.1016/j.engstruct.2011.07.011

[13.] Kelliher, D.; Sutton-Swaby, K.: Stochastic representation of blast load damage in a reinforced concrete building. Struct. Saf. 34(1),407–417 (2012). https://doi.org/10.1016/j.strusafe.2011.08.001

[14.] Abdollahzadeh, G.; Faghihmaleki, H.: Seismic-explosion riskbased robustness index of structures. Int. J. Damage Mech. 26(4), 523–540 (2017). https://doi.org/10.1177/1056789516651919

[15.] Syed, Z.I.; Mohamed, O.A.; Murad, K.; Kewalramani, M.: Performance of earthquake-resistant rcc frame structures under blast explosions. Procedia Engineering 180, 82–90 (2017)

[16.] Sevim, B.; Toy, A.T.: Blasting response of a two-storey rc building under different charge weight of tnt explosives. Iran. J. Sci. Technol. Trans. Civ. Eng. 44(2), 565–577 (2019)

[17.] Yusof, M.A.; Rosdi, R.N.; Nor, N.M.; Ismail, A.; Yahya, M.A.; Peng, N.C.: Simulation of reinforced concrete blast wall subjected to air blast loading. J. Asian Sci. Res. 4(9), 522–533 (2014)

[18.] Toy, A.T.; Sevim, B.: Numerically and empirically determination of blasting response of a RC retaining wall under TNT explosive. Adv. Concr. Constr. 5(5), 493–512 (2017). https://doi.org/10.12989/acc.2017.5.5.493

[19.] Andreou, M.; Kotsoglou, A.; Pantazopoulou, S.: Modelling blast effects on a reinforced concrete bridge. Adv. Civ. Eng. 2016, 1–11 (2016). https://doi.org/10.1155/2016/4167329

[20.] Hu, Z.-J.; Wu, L.; Zhang, Y.-F.; Sun, L.: Dynamic responses of concrete piers under close-in blast loading. Int. J. Damage Mech. 25(8),1235–1254 (2016). https://doi.org/10.1177/1056789516653245

[21.] Chen, J.; Liu, X.; Xu, Q.: Numerical simulation analysis of damage mode of concrete gravity dam under close-in explosion. KSCE J. Civ. Eng. 21(1), 397–407 (2017). https://doi.org/10.1007/s12205-016-1082-4

[22.] TEC (2018). Turkish Earthquake Code, Disaster and Emergency Management Presidency, Ankara, Turkey.

[23.] ANSYS Workbench (2016), Swanson Analyses System, Ansys Inc, USA

[24.] ANSYS Autodyn (2016), Swanson Analyses System, Ansys Inc, USA